

## Collisional broadening and shift of neutral argon spectral lines\*

D. P. Aeschliman and R. A. Hill

Sandia Laboratories, Albuquerque, New Mexico 87115

D. L. Evans

Arizona State University, Tempe, Arizona 85281

(Received 25 February 1976)

The collisional self-broadening and shift of neutral argon spectral lines have been determined as a function of atom density  $N$  for several lines terminating on either the lower resonance or lower metastable levels. The lines were emitted by a variable-pressure discharge tube equipped with intracapillary thermocouples, and were observed using a pressure-scanned Fabry-Perot interferometer. The line profiles were analyzed using a least-squares fit of Whiting's Voigt function to all profile intensity points. Particular attention was given to the determination of the gas temperature, from which  $N$  was calculated. The contribution of nonresonant interactions to the broadening and shift of lines connected to the ground state via resonant transitions was examined using the analysis of Lewis.

### I. INTRODUCTION

Collisional broadening and shift parameters of selected spectral lines in neutral argon have been obtained by several authors.<sup>1-5</sup> Such data have been used to infer resonant transition oscillator strengths of optically inaccessible lines,<sup>3</sup> and to account for the small effects of neutral collisions on measured widths and shifts in high-temperature, ionized argon flows where Doppler and Stark effects are the principal broadening and shift mechanisms.<sup>6</sup> (At the experimental conditions described in this paper, Stark effects are entirely negligible.) Broadening and shift parameters,  $2\gamma$  and  $\beta$ , respectively, are obtained from the slope of a plot of Lorentz width  $W_l$ , or shift  $W_s$  (i.e., allowing for Doppler and instrumental effects), versus neutral-atom density  $N$  for densities and temperatures for which the impact approximation is valid.<sup>7</sup>  $N$  is difficult to measure directly in a low-pressure dc discharge, the typical spectral-line emission source, although Rzhevskii<sup>8</sup> has recently shown pulsed holographic interferometry to be a promising technique. Therefore  $N$  has commonly been inferred from the pressure, temperature, and equation of state.<sup>1-3</sup> The pressure in a dc discharge is typically measurable to an accuracy of a few percent. The atom temperature  $T_a$ , however (except in a special high-temperature, high-pressure case reported by Copley and Camm<sup>4</sup>), has been inferred from measurements of the discharge-tube wall temperature  $T_w$  with the assumption that  $T_a = T_w$ . An analysis by Golubovskii *et al.*,<sup>9</sup> indicates that the validity of this assumption depends on the discharge-tube diameter, pressure, and current. The results of Ref. 9 have been qualitatively confirmed by Rzhevskii,<sup>8</sup> as well as by the results of this study. Thus based on the

calculations of Ref. 9 and the experimental results obtained at identical discharge conditions by Rzhevskii<sup>8</sup> the results of Hindmarsh and Thomas<sup>1,2</sup> for  $2\gamma$  and  $\beta$  for the Ar I 6965-Å line, for example, appear to be  $\approx 15\%$  low as a result of the assumption of equal atom and wall temperatures.

In this paper, new measurements of the neutral argon broadening and shift parameters are reported for eight near-infrared lines ( $4p-4s$ , 6677  $\leq \lambda \leq 8104$  Å) and one blue line ( $5p-4s$ ,  $\lambda 4159$ ) in the argon spectrum. The shift parameters are given for four additional lines whose broadening was seriously influenced by self-absorption. These results are based on measured atom temperatures, since Golubovskii *et al.*<sup>9</sup> predicted substantially elevated  $T_a$  for the conditions of this experiment. The  $4s$  levels upon which the observed lines terminate are the lower metastable level ( $^2P_{3/2}4s[\frac{3}{2}]_2$ ) and the upper level ( $^2P_{3/2}4s[\frac{3}{2}]_1$ ) of the weaker resonance line. The upper levels ( $4p$ ,  $5p$ ) are perturbed by Van der Waals interactions ( $C_6/r^6$  potential, where  $r$  is the intermolecular separation). The resonant level is perturbed by the longer-range ( $C_3/r^3$  potential) resonant interaction with the ground state. Both of these effects are proportional to atom density  $N$ .<sup>7,10</sup> The lower metastable level is presumed to be perturbed only weakly, if at all, by collisional processes.

In addition to collisional effects directly proportional to  $N$ , lines broadened only by Van der Waals interactions (i.e., those leading to a nonresonant level) possess a  $T_a^{0.3}$  dependence for  $2\gamma$  and  $\beta$ , as predicted theoretically by Foley<sup>7</sup> and Lindholm.<sup>10</sup> For this case, these theories predict  $2\gamma/\beta = 2.76$ , independent of both  $T_a$  and  $N$ .

Phase-shift theory<sup>7</sup> predicts that lines terminating on resonant levels that involve strong reso-

nant coupling to the ground state will be broadened but unshifted. This is observed experimentally<sup>3</sup> for the Ar I 7503-Å line, for example. It is also predicted and observed that the resonance broadening of such lines exhibits no temperature dependence. Lines such as Ar I 7273, however, whose lower state is coupled more weakly to the ground state, is noticeably shifted due to the presence of the Van der Waals (VdW) interaction.

Lewis,<sup>11</sup> assuming that the individual contributions to the phase shifts from the resonant and dispersion (VdW) interactions are additive, has derived the neutral broadening and shift for the case of comparable resonant and Van der Waals interactions. His solutions will be used here to determine the resonance contribution to the broadening, from which the resonant line oscillator strength  $f_{jj'}$  can be obtained from the relation<sup>3</sup>

$$2\gamma = k_{jj'}(e^2 f_{jj'}/8mc^2 v_{jj'})N. \quad (1)$$

In Eq. (1)  $m$  is the electron mass,  $v_{jj'}$  is the wave number of the resonant transition,  $k_{jj'}$  is a constant, and  $e$  and  $c$  have their usual meanings. The constant  $k_{jj'}$  depends on the  $j$  values of the resonant and ground states; recent theory,<sup>12</sup> supported by measurement of  $f_{jj'}$  in helium,<sup>13</sup> indicates  $k_{jj'} = 1.45$ .

Although Lewis<sup>11</sup> considers his theory for the shift in the presence of comparable resonant and Van der Waals interactions to be more speculative than for the widths, we will also compare the observed shifts to his predictions for the same pairs of spectral lines.

## II. EXPERIMENTAL TECHNIQUE

The experimental arrangement is shown in Fig. 1. Light emitted by a variable-pressure, direct-

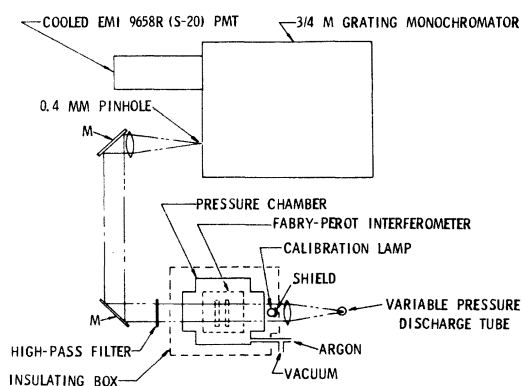


FIG. 1. Experimental apparatus. A high-pass filter that transmits wavelengths longer than 5000 Å was removed for measurements at  $\lambda 4159$ .

current discharge tube (VPDT), depicted in greater detail in Fig. 2, is collimated by a lens and passed through a plane Fabry-Perot interferometer (FPI). The FPI plates were enclosed in an Invar-36 holder of 55 mm aperture. This holder was mounted in a thick-walled evacuable brass cylinder that permitted external adjustment of the plate parallelism; the entire assembly was enclosed in an insulated chamber to eliminate spectral drift due to laboratory temperature variations over typical run times (10–20 min). Parameters describing the FPI are listed in Table I. The center of the interference pattern of the VPDT radiation was focused on a 400- $\mu\text{m}$ -diam pinhole that served as the entrance aperture for the monochromator. The monochromator, with an exit slit width of 400  $\mu\text{m}$ , provided a total spectral band pass of about 5 Å, and served to isolate a given spectral line for analysis. Higher-order radiation from the 1200-lines/mm grating was eliminated with a high-pass filter.

In the manner of Jacquinet and Dufour,<sup>14</sup> spectral scanning was accomplished by varying the pressure, and thus the index of refraction, of argon gas in the FPI housing. Argon gas was introduced into the FPI through a choked needle valve, thus ensuring a linear rate of pressure change; pres-

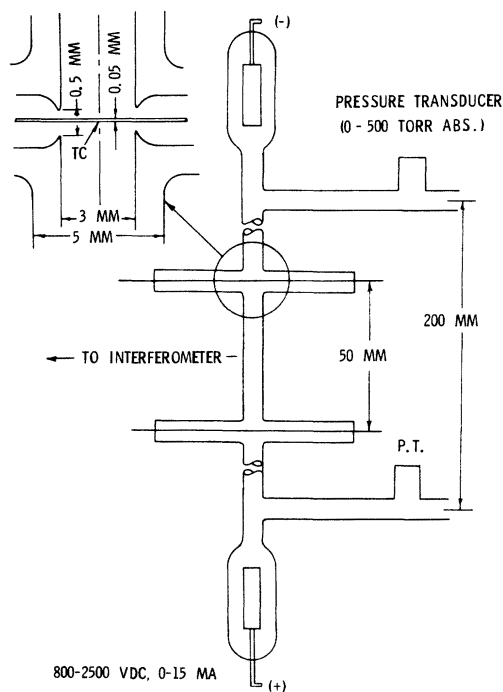


FIG. 2. Variable-pressure discharge tube (VPDT). Atom temperature was measured with chromel-alumel thermocouples (TC) situated in the discharge on either side of the viewing location.

TABLE I. FPI parameters ( $\lambda = 7273 \text{ \AA}$ ).

Diameter	60.0 mm
Clear aperture	55.0 mm
Plate thickness	15.0 mm
Flatness	$\lambda/200$
Wedge angle	0.5 deg
Coating	Multilayer dielectric
Spacing	10.36 mm
Reflectivity	>99%
Transmission	0.2%
$L_c$ focal length (see Fig. 1)	330 mm
Measured finesse	65
Free spectral range	0.2553 $\text{\AA}$

tures were measured with a precision strain-gauge transducer and recorded on both a digital computer and on one channel of a two-pen strip-chart recorder. Line profile intensities from the VPDT were also recorded by digital computer and displayed on the second channel of the strip-chart recorder.

The flow rate of argon through the VPDT was adjusted so that the pressure drop through the 3-mm-i.d. capillary, as determined by precision temperature-compensated strain-gauge transducers on the inlet and exhaust ports, was negligible compared to the average VPDT gas pressure. Flow rates were sufficient, however, to permit stable gas temperatures to be achieved in times  $\leq 1$  min following a change in VPDT pressure or current. Maximum uncertainty in average pressure was  $\pm[0.5 \text{ Torr} + (1\% \text{ of reading})]$ .

The atom temperature  $T_a$  was measured with an electrically floating chromel-alumel thermocouple (TC) located on the capillary axis, as shown in Fig. 2. Typical values are shown in Fig. 3 for several VPDT pressures and currents, along with gas temperatures based on the apparent Doppler width of the spectral line (see Sec. III). The calculations of Golubovskii *et al.*<sup>9</sup> for the discharge tube conditions ( $2 \leq P \leq 80 \text{ Torr}$  and  $3 \leq I \leq 15 \text{ mA dc}$ ) indicate that radial gradients in VPDT gas temperature were small. Rzhevskii<sup>8</sup> indicates somewhat larger gradients at the higher pressures and currents. In these cases, however, the diameter of the luminous column is constricted and the total variation in  $T_a$  over the radiating volume is small. Errors in  $T_a$  due to thermal conduction through the lead wires were estimated by running identical discharges in the presence of lead wires varying from 0.005 to 0.024 cm diameter. Effects of lead wire size were more noticeable at higher pressures, consistent with Rzhevskii's observations. However, maximum errors in  $T_a$  due to thermal conduction losses are estimated to be less than  $10^\circ\text{C}$ , and total errors in the  $T_a$  measurements are estimated to be less than  $20^\circ\text{C}$ . Gas

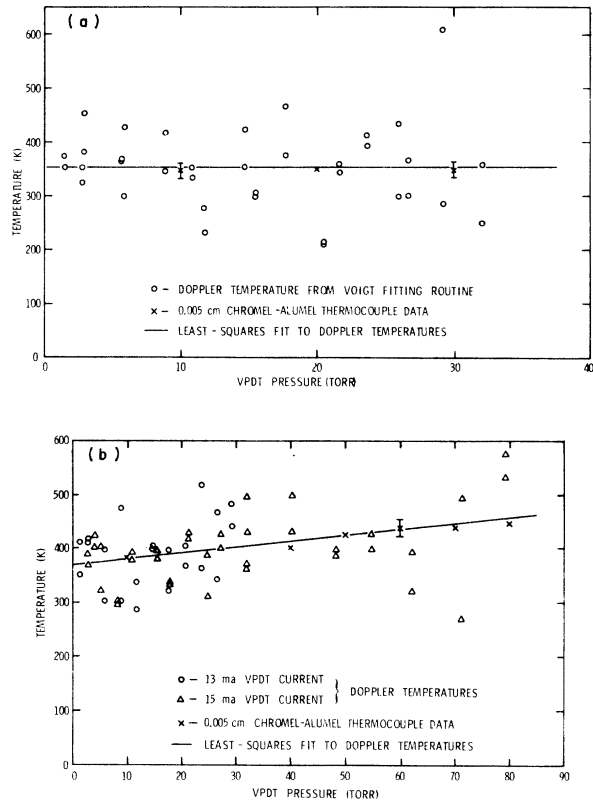


FIG. 3. (a) VPDT atom temperatures vs discharge pressure at low discharge current ( $I \leq 5 \text{ mA dc}$ ).

(b) VPDT atom temperatures vs discharge pressure at high discharge current ( $I \geq 13 \text{ mA dc}$ ).

densities in the center of the capillary were obtained from the measured pressure and temperature and equation of state,  $N = P/kT_a$ .  $N$  varied from  $\sim 5 \times 10^{16} \text{ cm}^{-3}$  at  $\sim 2 \text{ Torr}$  to  $\sim 1.8 \times 10^{18} \text{ cm}^{-3}$  at  $\sim 80 \text{ Torr}$ . Loss of pressure measurement accuracy at low pressures, and erratic discharge behavior at high pressures, limited the pressure range. Over the range of VPDT pressure and current noted above, the FPI pressure and the neutral argon spectral-line profiles, consisting of typically 30 to 50 intensities, were recorded by a digital computer. A fixed-wavelength reference for each line was provided by a constant-pressure discharge tube ("calibration lamp") placed in the parallel beam inside the insulating chamber, as shown in Fig. 1; the linear relation between FPI pressure and transmitted wavelength was established by scanning the FPI over several free spectral ranges for each line.

### III. LINE PROFILE ANALYSIS

The line profiles were analyzed using an approximate Voigt function given by Whiting,<sup>15</sup>

$$I_\lambda = I_{\lambda_0} \left( \left( 1 - \frac{W_l}{W_v} \right) \exp \left[ -2.772 \left( \frac{\lambda - \lambda_0}{W_v} \right)^2 \right] + \left( \frac{W_l}{W_v} \right) \frac{1}{1 + 4 \left[ (\lambda - \lambda_0) / W_v \right]^2} + 0.016 \left( 1 - \frac{W_l}{W_v} \right) \left( \frac{W_l}{W_v} \right) \right. \\ \left. \times \left\{ \exp \left[ -0.4 \left( \frac{\lambda - \lambda_0}{W_v} \right)^{2.25} \right] - \frac{10}{10 + \left[ (\lambda - \lambda_0) / W_v \right]^{2.25}} \right\} \right), \quad (2)$$

where  $I_\lambda$  is the intensity at wavelength  $\lambda$  and  $W_v$  and  $W_l$  are the Voigt and Lorentz full widths at half-maximum, respectively. Except for four cases noted below, all intensity points comprising each profile were fitted by least squares with Eq. (2). Spectral-line profile overlap from adjacent free spectral ranges was included to all orders. In the fitting routine,  $W_v$ ,  $W_l$ , and the line center  $\lambda_0$  were varied in an iterative scheme that minimized the sum of the squares of the residuals.  $I_{\lambda_0}$ , the intensity at the line center, is a scale factor obtained in the fit that normalizes the areas of the experimental and analytical profiles.

Representative Ar I 7273-Å line profiles, for several VPDT pressures, and the calibration lamp profile are shown in Fig. 4. The line through each profile is the best Voigt fit as defined by Eq. (2). Standard deviations, scaled to the profile peak height, were typically a few percent or less, part of which was due to the inherent inaccuracies in Eq. (2),<sup>16</sup> with the remainder due to the noise in the intensity data and, possibly, to minor departures of the experimental profiles from Voigt shape.

The Gaussian (Doppler) full widths at half-maximum,  $W_g$ , were calculated with values obtained above for  $W_v$  and  $W_l$  using the expression<sup>15</sup>

$$W_g = [W_v(W_v - W_l)]^{1/2}. \quad (3)$$

These widths were used to calculate values of the gas temperature

$$T_a = 7.79 \times 10^{13} (W_g^2 / \lambda_0^2), \quad (4)$$

(for argon) shown in Fig. 3. A least-squares regression analysis of these temperature data, as a function of discharge-tube pressure and current, agrees to within a few percent with the thermocouple temperature measurements. Based on this agreement, a value of  $T_a$  was established for each line profile with the empirical expression

$$T_a = 353, \quad I_D \leq 5 \text{ mA dc},$$

$$T_a = 353 + 0.12 P_D (I_D - 5), \quad I_D > 5 \text{ mA dc}, \quad (5)$$

where  $P_D$  is the discharge-tube pressure in Torr and  $I_D$  is the discharge-tube current in mA dc. These calculated values of  $T_a$ , in conjunction with Eqs. (3) and (4), were then used in a modified version of the profile fitting routine which iterated on

$W_v$  and  $\lambda_0$  only.

Spectral lines possessing large  $Ag$  products ( $A$  is the transition probability,  $g$  the statistical weight of upper level), and terminating on the metastable level,<sup>17</sup> were observed to be significantly self-absorbed. For these lines, Voigt-function fits and the application of Eqs. (3) and (4) yielded values of  $T_a$  consistently too high by factors of up to 5, even though apparently good fits were obtained, i.e., fits with low standard deviations. Efforts to reconstruct the line emission profiles were not successful; hence for such lines we report only the shift parameters.

#### IV. RESULTS

Representative plots of  $W_l$  vs  $N$  and  $W_s$  vs  $N$  for several optically thin neutral argon lines appear in Figs. 5 and 6.  $2\gamma$  and  $\beta$  ( $dW_l/dN$  and  $dW_s/dN$ )

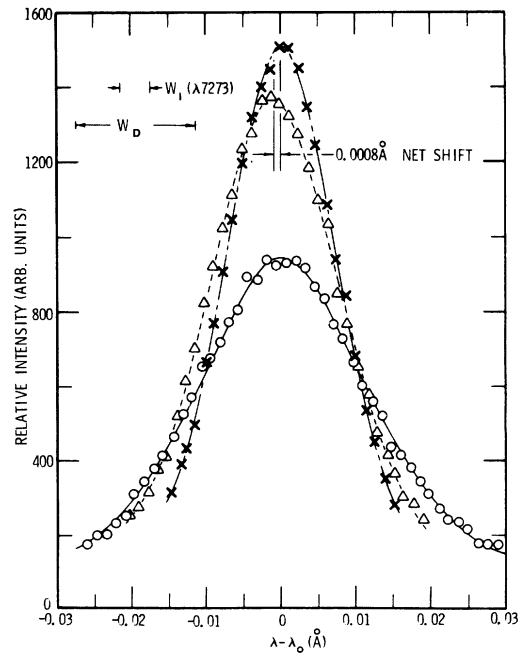


FIG. 4. Representative Ar I 7273-Å line profiles.  $\times$ : calibration lamp;  $\Delta$ : VPDT at 11.0 Torr and 15 mA dc ( $T_a = 366 \pm 20$  K);  $\circ$ : VPDT at 32.0 Torr and 15 mA dc ( $T_a = 391 \pm 20$  K). The calibration lamp has a net red shift of  $\sim 0.0014$  Å relative to the zero-density intercept of VPDT shift data; hence the apparent shift of the 11-Torr profile is negative.

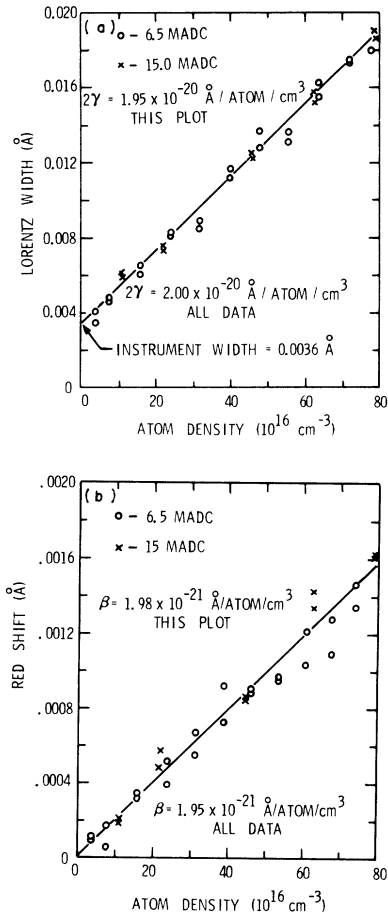


FIG. 5. (a) Lorentz width  $W_L$  vs atom density for Ar I 7273-Å line for 6.5- and 15.0-mA dc discharges. (b) Red shift  $W_s$  vs atom density for Ar I 7273-Å line for conditions of Fig. 5(a). Net shift of calibration lamp has been added to all values to yield zero shift at zero density.

$dN$ , respectively) were obtained for the optically thin lines directly from least-squares regression analysis of width or shift vs  $N$ . Only  $\beta$  was obtained for the self-absorbed lines. These results are presented in Table II, with results from other investigators where available. Here, the results for  $2\gamma$  for lines terminating on the resonant level include the small (1–2%) contribution due to non-resonant interactions. The indicated uncertainties include both statistical and estimated systematic errors. As noted previously,  $\beta$  should not be affected by self-absorption; hence the shift data were analyzed as though the lines were optically thin. No systematic dependence of  $\beta$  on  $I_D$  or  $P_D$  was apparent in any of the data.

The apparent instrument widths  $W_I(\lambda)$  were obtained by extrapolating  $W_L$  vs  $N$  to zero density, assuming no "extrapolation anomaly."<sup>13,18</sup> These vary widely due to the variation in FPI plate re-

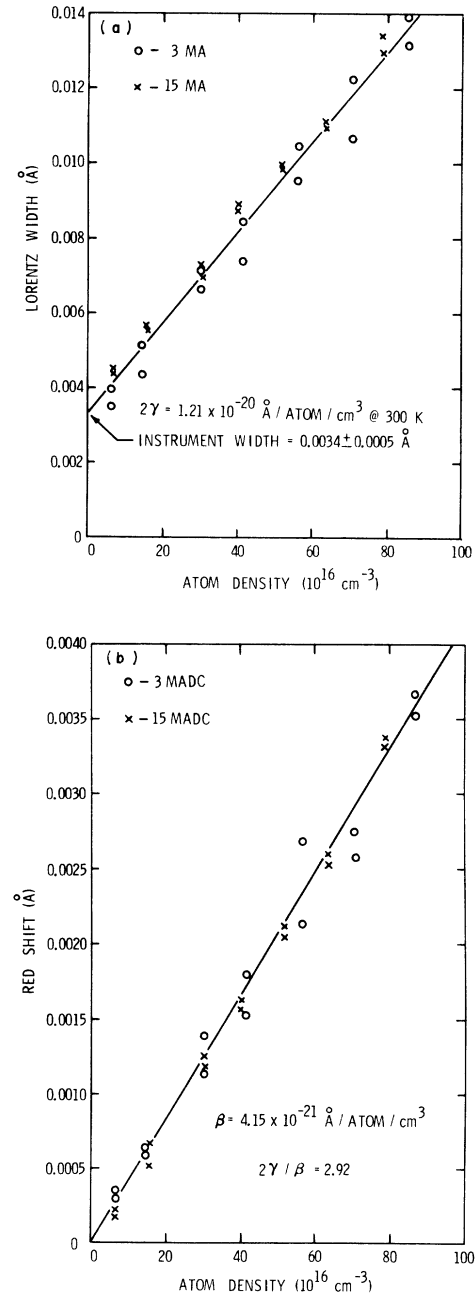


FIG. 6. (a) Lorentz width vs atom density for Ar I 7147-Å line for 3.0- and 15.0-mA dc discharges. Collisional contribution to each width value was corrected to 300 K prior to obtaining  $2\gamma$ . (b) Red shift vs atom density for Ar I 7147-Å line for conditions of Fig. 6(a). Data corrected to 300 K.

flectivity  $R$ . Here we have assumed the instrument broadening function to be Lorentzian.<sup>19</sup> This is a good approximation provided that the reflectivity, through the Airy function, is the dominant factor controlling the instrumental broadening.

TABLE II. Argon collisional broadening and shift parameters,  $2\gamma$  and  $\beta$ .

Line (Å)	Lower level <sup>a</sup>	$2\gamma^b$ ( $10^{-20}$ Å/atom cm <sup>3</sup> )		$\beta^b$ ( $10^{-21}$ Å/atom cm <sup>3</sup> )		$2\gamma/\beta$	
		This work	Other data	This work	Other data	This work	Other data
4158.59	Met.	1.20 ± 0.06		3.44 ± 0.15		3.49	
6677.28	Res.	1.79 ± 0.09		2.30 ± 0.10		7.78	
6965.43	Met.		0.808, <sup>c</sup> 1.403 <sup>d</sup> 0.910, <sup>e</sup> 0.968 <sup>f</sup>	3.77 ± 0.20	2.31, <sup>e</sup> 3.65, <sup>e</sup> 3.14 <sup>g</sup>		3.5, <sup>c</sup> 2.5 <sup>e</sup>
7067.21	Met.	0.913 ± 0.090	1.45, <sup>d</sup> 0.973 <sup>e</sup>	3.56 ± 0.50	3.05, <sup>g</sup> 4.22 <sup>e</sup>	2.56	2.3 <sup>e</sup>
7147.16	Met.	1.18 ± 0.06		3.87 ± 0.20		3.05	
7272.94	Res.	2.00 ± 0.10	1.85, <sup>c</sup> 2.16 <sup>e</sup>	1.95 ± 0.10		10.3	
7383.98	Res.	1.55 ± 0.30	2.19 <sup>e</sup>	1.53 ± 0.15		10.1	$f = 0.068 \pm 0.007$ (this work)
7471.16	Res.	2.56 ± 0.50		3.54 ± 0.70		7.23	
7514.65	Res.	1.71 ± 0.40	1.94, <sup>c</sup> 2.41 <sup>e</sup>	1.96 ± 0.10		8.72	
7635.10	Met.		1.40 <sup>d</sup>	4.98 ± 0.25			
8006.15	Res.	2.27 ± 0.25	2.60 <sup>e</sup>	2.37 ± 0.12		9.58	
8014.79	Met.		1.25 <sup>e</sup>	5.11 ± 0.25	4.03 <sup>e</sup>		3.1 <sup>e</sup>
8103.67	Res.	2.44 ± 0.50	2.82 <sup>e</sup>	2.25 ± 0.10		10.8	
8115.31	Met.			4.73 ± 0.25			

<sup>a</sup> Metastable (Met.) or resonant (res.) levels.

<sup>b</sup> Observed value reduced to 300 K using Foley-Lindholm  $T^{0.3}$  dependence for lines terminating on metastable level.

<sup>c</sup> Reference 3.

<sup>d</sup> C. S. Lee, D. M. Camm, and G. H. Copley, J. Quant. Spectrosc. Radiat. Transfer **15**, 211 (1975).

<sup>e</sup> Reference 4.

<sup>f</sup> Reference 1.

<sup>g</sup> Reference 2.

According to Hernandez,<sup>20</sup> the broadening function due to microscopic flatness imperfections is generally Gaussian, and that from both spherical curvature and the finite aperture is rectangular. For the plates used, deviations from microscopic flatness imperfections and from spherical curvature are less than  $\lambda/200$  at 7273 Å. Hence the contribution to  $W_g$  through the Gaussian term is negligible compared to the Doppler contribution  $W_D$  (since  $W_g^2 = W_D^2 + W_{imp}^2$ , where  $W_{imp}$  is the total half-width due to plate imperfections) and the rectangular contribution is negligible compared to the width of the Airy function except at the highest values of reflectivity, where they become comparable. For these cases, however, the ratio  $W_I(\lambda)/W_I(\lambda) \ll 1$  and the net error in  $W_I$  from this source is small. Figure 7 shows the FPI plate transmission  $\tau$  and the instrument width  $W_I(\lambda)$  as functions of  $\lambda$ . Assuming that the reflectivity  $R = 1 - \tau$  (i.e., neglecting any absorption losses in the plate coatings),  $W_I(\lambda)$  should, and does, vary directly with  $\tau$  except at the longest wavelengths, where the assumption of negligible absorption may be invalid.

For lines terminating on the metastable level (Van der Waals broadening only), the theoretical Foley-Lindholm<sup>7,10</sup>  $T^{0.3}$  temperature dependence was used to adjust the  $W_I$  and  $W_s$  data to 300 K prior to obtaining  $2\gamma$  and  $\beta$ . According to Lewis,<sup>11</sup>

the temperature dependence of the lines terminating on the weaker resonant level is very small and thus has not been included.

The width data for the Ar I 7273-Å line, which terminates on the lower resonance level, and the Ar I 6965-Å line,<sup>3</sup> which originates from the same upper state, but terminates on the metastable level, have been used to obtain the resonant transition oscillator strength  $f_{jj}$ , [Eq. (1)] using a  $k_{jj}$  of 1.45. Lewis's theory<sup>11</sup> was used to account for

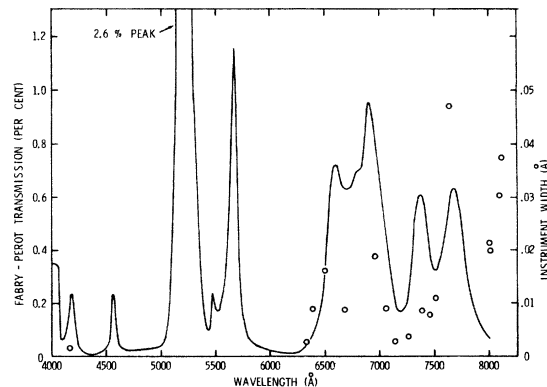


FIG. 7. Fabry-Perot transmission and instrument width (○) vs wavelength. The assumption of negligible absorption is probably not valid above 8000 Å (see text).

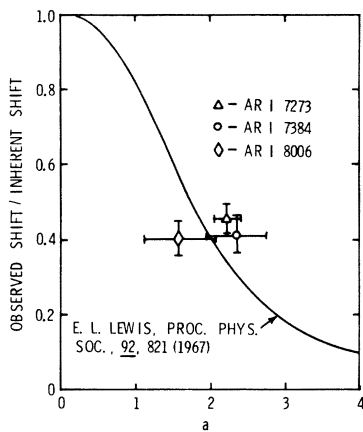


FIG. 8. Ratio of observed shift to inherent shift vs  $a [= 2\gamma(3)/2\gamma(6)]$  for several Ar I lines terminating on the resonance level.

the small effect due to nonresonant interactions. The value for  $f_{jj}$ , obtained is  $0.068 \pm 0.007$ , in good agreement with the value  $0.059 \pm 0.003$  obtained from radiative lifetime measurements,<sup>21</sup> and

$0.063 \pm 0.004$  obtained by Lewis<sup>11</sup> using the Ar I 7273- and 6965-Å broadening data of Stacey and Vaughan.<sup>3</sup>

The shift ratios  $\beta_{\lambda 7273}/\beta_{\lambda 6965}$ ,  $\beta_{\lambda 7384}/\beta_{\lambda 7067}$ , and  $\beta_{\lambda 8006}/\beta_{\lambda 7635}$  were compared to Lewis's solution for the shift reduction of lines perturbed by comparable Van der Waals and resonant interactions. Here we have assumed  $2\gamma = 2.76\beta$  to obtain the width for the strongly self-absorbed Ar I 7635-Å line. The results are shown in Fig. 8, where the solid curve is reproduced from Fig. 2 of Lewis's paper.<sup>11</sup>

The agreement for these lines is as good as could be expected in view of Lewis's reservations about his calculation for the shifts, and the uncertainties in  $a [= 2\gamma(3)/2\gamma(6)]$ , Lewis's notation]. Lewis indicates that the choice of cutoff in the phase-shift integral is both more uncertain and more critical than in the broadening calculation. The vertical error bars on the data shown in Fig. 8 indicate the estimated uncertainty in the measured shift ratios; the horizontal error bars give the range in  $a$  corresponding to the range of estimated uncertainty in the measured broadening parameters, assuming his theory to be exact.

\*Work supported by the U.S. Energy Research and Development Administration.

<sup>1</sup>W. R. Hindmarsh and K. A. Thomas, Proc. Phys. Soc. Lond. A **77**, 1193 (1961).

<sup>2</sup>W. R. Hindmarsh and K. A. Thomas, Mon. Not. R. Astron. Soc. **119**, 21 (1959).

<sup>3</sup>D. N. Stacey and J. M. Vaughan, Phys. Lett. **11**, 105 (1964).

<sup>4</sup>G. H. Copley and D. M. Camm, J. Quant. Spectrosc. Radiat. Transfer **14**, 899 (1974).

<sup>5</sup>D. M. Camm and F. L. Curzon, Can. J. Phys. **50**, 2866 (1972).

<sup>6</sup>D. P. Aeschliman and D. L. Evans, J. Quant. Spectrosc. Radiat. Transfer **16**, 191 (1976).

<sup>7</sup>H. M. Foley, Phys. Rev. **69**, 616 (1946).

<sup>8</sup>V. N. Rzhavskii, Opt. Spektrosk. **37**, 1168, 1974 [Opt. Spectrosc. **37**, 671 (1974)].

<sup>9</sup>Yu. B. Golubovskii, Yu. M. Kagan, and L. L. Komarova, Cpt. Spektrosk. **35**, 8, 1973 [Opt. Spectrosc. **35**, 16 (1973)].

<sup>10</sup>E. Lindholm, Arkiv Mat. Astron. Fys. A **32**, 1 (1946).

<sup>11</sup>E. L. Lewis, Proc. Phys. Soc. Lond. **92**, 817 (1967).

<sup>12</sup>A. Omont, C. R. Acad. Sci. Paris B **262**, 190 (1966).

<sup>13</sup>J. M. Vaughan, Proc. R. Soc. A **295**, 164 (1966).

<sup>14</sup>P. Jacquinet and C. Dufour, J. Rech. Cent. Natl. Rech. Sci. Lab. Bellevue (Paris) No. 6, 91 (1948).

<sup>15</sup>E. E. Whiting, J. Quant. Spectrosc. Radiat. Transfer **8**, 1379 (1968).

<sup>16</sup>Whiting (Ref. 15) indicates that the errors in  $I_\lambda/I_{\lambda_0}$  range from -5.0 to +2.5%, and the error in  $W_0$  is less

than 1% throughout the range from pure Gaussian to pure Lorentzian profiles. An exact method for obtaining computer fits to a Voigt profile from a scanning Fabry-Perot interferometer has been described by R. C. Sze and W. R. Bennett, Jr., Phys. Rev. A **5**, 837 (1972). This method requires that the plate reflectivity and the mathematical functions describing other FPI broadening mechanisms (e.g., plate defects, misalignment, aperture broadening) be known as a function of wavelength. This method also requires the background continuum radiation (or noise levels) to be accurately known, or negligible. Errors in Lorentz width incurred through the use of Whiting's analytic approximation to the Voigt function are expected to be small relative to experimental sources of error.

<sup>17</sup>The reduced electron density leads to overpopulation of the metastable level, since collisional excitation is the only effective depopulation mechanism. Consistent with this is the fact that self-absorption is observed to be more pronounced at lower discharge current (lower electron density).

<sup>18</sup>A. R. Malvern, J. L. Nicol, and D. N. Stacey, J. Phys. B **7**, L518 (1974). These authors suggest that the so-called extrapolation anomaly is due to a non-Maxwellian velocity distribution function that persists at low densities following exciting collisions.

<sup>19</sup>R. A. Day, Appl. Opt. **9**, 1213 (1970).

<sup>20</sup>G. Hernandez, Appl. Opt. **5**, 1945 (1966).

<sup>21</sup>G. M. Lawrence, Phys. Rev. **175**, 40 (1968).